Pure Appl. Chem., Vol. 76, Nos. 7–8, pp. 1309–1319, 2004.

Block copolymer vesicles*

Joost A. Opsteen, Jeroen J. L. M. Cornelissen‡, and Jan C. M. van Hest

Department of Organic Chemistry, NSRIM Institute, University of Nijmegen, Toernooiveld 1, 6525 ED Nijmegen, The Netherlands

Abstract: Amphiphilic block copolymers have the ability to assemble into multiple morphologies in solution. Depending on the length of the hydrophilic block, the morphology can vary from spherical micelles, rods, and vesicles to large compound micelles (LCMs). Vesicle formation is favored upon an increase in total molecular weight of the block copolymer, that is, an increasing bending modulus (K). Owing to the polymeric character of this type of vesicle (also called polymersomes), they possess remarkable properties. The diffusion of (polymeric) amphiphiles in these vesicles is very low compared to liposomes and for high-molecular-weight chain entanglements even lead to reptation-type motions, which make it possible to trap near-equilibrium and metastable morphologies. Additionally, in contrast to liposomes, membrane thicknesses can exceed 200 nm. As a consequence, this increased membrane thickness, in combination with the conformational freedom of the polymer chains, leads to a much lower permeability for water of block copolymer vesicles compared to liposomes. The enhanced toughness and reduced permeability of polymersomes makes them, therefore, very suitable as stable nanocontainers, which can be used, for example, as reactors or drug delivery vehicles.

Self-assembly of amphiphilic block copolymers in solution has been a topic of active research for more than 30 years. The most commonly observed morphology in these systems is the star-micelle. "Star" refers to the fundamental core-corona structure, which consists of a small core and a large corona. These star-micelles can be divided into regular and reversed micelles, which are formed in polar and apolar solvents, respectively.

Over the past few years, the ability of highly asymmetric, amphiphilic block copolymers to assemble into aggregates of multiple morphologies in solution has attracted much attention. For these "crew-cut" aggregates, a term proposed by Halperin et al. [1], the longer block forms the core of the aggregate, while the corona is composed of the short segment. Manipulation of the relative block lengths and environmental parameters, such as solvent composition, the presence of additives, and temperature, has resulted in a variety of morphologies, including spheres, rods, vesicles, lamellae, tubules, large compound micelles (LCMs), large compound vesicles (LCVs), and hexagonally packed hollow hoops (HHHs).

Several of these block copolymer morphologies are classified as vesicles because they all have hollow-spherical structures containing walls composed of bilayers of polymer molecules. The field of block copolymer vesicles (polymersomes) has only recently been explored. The earliest reports on polymersomes focused on vesicles prepared from bulk copolymer systems [2] and block copolymer/homo-

*Lecture presented at the symposium "Controlling the self assembly in macromolecular systems: From nature to chemistry to functional properties", as part of the 39th IUPAC Congress and 86th Conference of the Canadian Society for Chemistry: Chemistry at the Interfaces, Ottawa, Canada, 10–15 August 2003. Other Congress presentations are published in this issue, pp. 1295–1603.
‡Corresponding author

polymer blends [3]. Over the past few years, it has been proven that vesicles can be prepared from a variety of block copolymers in different media, Fig. 1 [4,5].

As mentioned above, besides the formation of vesicles, asymmetric block copolymers are able to assemble into a variety of structures. The morphology of these aggregates is governed by a balance of contributions to the free energy of aggregation: (i) core-chain stretching, (ii) interfacial energy, and (iii) intercoronal chain interactions [1]. Thus, morphologies can be controlled by many factors which influence one or more of the three free-energy contributions. The influence of solvent conditions on block copolymer morphologies has been recently reviewed by Choucair and Eisenberg [20] and will, therefore, be excluded in this overview and focus will be on the influence of the block copolymer structure on the morphology.

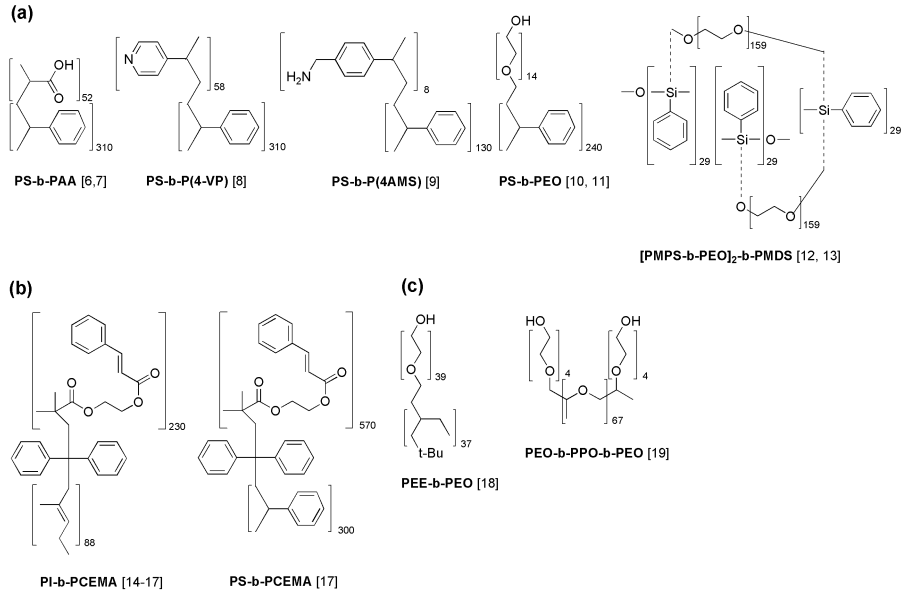

Fig. 1 Examples of vesicle-forming polymers in (a) solvent–water mixtures; (b) organic solvents; and (c) aqueous solution [6–19].

Block copolymer structure

Undoubtedly, the main factor controlling the morphology is the structure of the block copolymer. In order to obtain crew-cut type aggregates, the amphiphilic block copolymer needs to be highly asymmetric, i.e., comprised of long, hydrophobic core-forming blocks and short, hydrophilic corona blocks. However, the morphology of the different types of crew-cut aggregates is also governed by the composition of the block copolymer and will be discussed in the next two sections.

Hydrophilic block length dependence

The dependence of the corona block length on the morphology of crew-cut aggregates has been demonstrated by preparation of block copolymers with constant core-forming block lengths and varying corona chain lengths.

A series of colloidal dispersions of polystyrene-*block*-poly(acrylic acid) (PS-*b*-PAA) in DMF/water mixtures has been prepared under conditions of near thermodynamic equilibrium, and subsequently dialyzed against distilled water in order to remove DMF. With decreasing corona-forming PAA block lengths, the morphology changes from spherical to rod-like micelles, to vesicles, and to micrometer-size spheres, respectively (Fig. 2) [21].

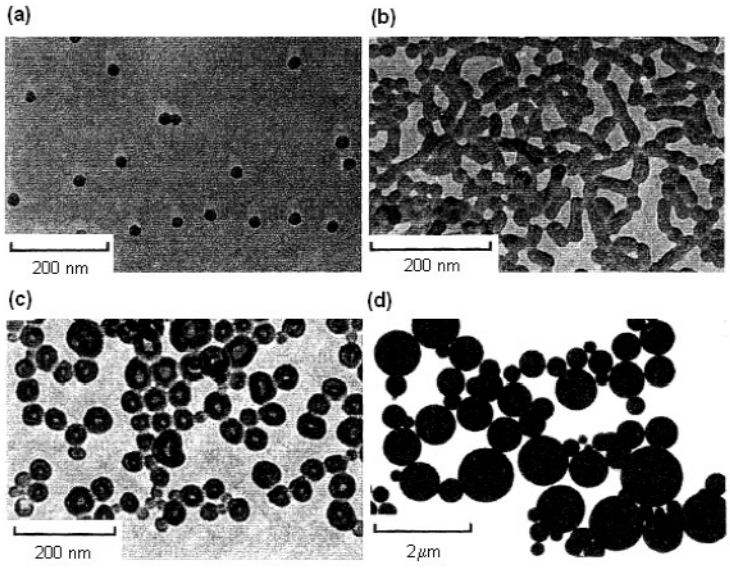

Fig. 2 TEM images of multiple morphologies of crew-cut aggregates of PS-*b*-PAA block copolymers: (a) PS_{200}-*b*-PAA_{21} spherical micelles; (b) PS_{200}-*b*-PAA_{15} rod-like micelles; (c) PS_{200}-*b*-PAA_{8} vesicles; and (d) PS_{200}-*b*-PAA_{4} reversed micelles coexisting with up to micrometer-size spheres with hydrophilic surfaces and filled with reversed micelles. Reproduced from ref. [21] with permission from the AAAS.

With a relatively long PAA block, micelles are observed initially. When the PAA block length is decreased, the repulsive interactions between coronal block chains decrease, thus also the surface area per corona chain (A_c) decreases. Therefore, more chains can aggregate, leading to larger spheres. An increase in sphere radius leads to stretching of the PS chains, which implies that the larger the PS core, the higher the average degree of core-chain stretching (S_c) will be. This core-chain stretching is accompanied by a decrease in entropy. Consequently, when the aggregates become very large, the entropic penalty of the core-block stretching renders simple spheres unfavorable as a low-energy morphology. This leads to the formation of rod-like micelles with decreased core diameters, and a reduction in the degree of core-chain stretching. A decrease of the PAA block length to a greater extent results in an increase in rod diameter due to the decrease in inter-coronal repulsion. Ultimately, in the same manner as for the simple sphere-rod transition, the core-block stretching term will dictate a further morphological transition to vesicular structures [22].

These abovementioned observations are analogous to the theory of small-molecule surfactants [23,24], viz. as the PAA block length decreases, also the surface area per corona chain decreases. As a result, the value of the packing parameter ($v/a_o l_c$) will increase correspondingly. However, this may not be the primary reason for the occurrence of morphological transitions [5]. For micelles built up of small-molecule surfactants, the surface area per head group is mainly determined by the balance of forces between head group repulsion and hydrophobic attraction of the core surface. Changes in the stretching force of the hydrophobic chains are less important because the chains are stretched already. On the contrary, for the block copolymer crew-cut aggregates, the surface area per corona chain is largely dependent on the structure of the insoluble block (PS), the geometrical shape of the aggregates, and the length of the corona block (PAA) itself. The repulsion between the corona blocks is relatively unimportant because the blocks are short and acidic [22].

The same trend in morphological transition from spherical to bilayer aggregates with decreasing hydrophilic block length has also been observed in aqueous solutions of a very different diblock copolymer family, i.e., polystyrene-*block*-poly(ethylene oxide) (PS-*b*-PEO) [10].

A distinct class of amphiphilic macromolecules capable of vesicle formation has been synthesized by coupling of PS to poly(propylene imine) dendrimers [25]. The shape of these PS-dendrimer diblock copolymers is comparable with that of small-molecule surfactants, and not with the more traditional block copolymers described earlier. The geometry of these PS-dendrimer block copolymers is dependent on the generation of the dendrimer, as can be seen in Fig. 3. It has been shown that in aqueous phases, PS-dendr-$(NH_2)_{32}$ forms spherical micelles, PS-dendr-$(NH_2)_{16}$ forms micellar rods, and PS-dendr-$(NH_2)_8$ forms vesicular structures. This observed effect of amphiphile geometry on the aggregation behavior is in qualitative agreement with the theory of Israelachvili et al. [23], which related the amphiphile geometry to the formed morphology.

Explorative studies on block copolymers having a styrene segment and a helical polyisocyanide block, shown next to the formation of helical superstructures, also the existence of bilayer type aggregates and vesicles. These structures were only found when the ratio between the hydrophobic polystyrene and the hydrophilic dipeptide-based polyisocyanide blocks was optimized [26]. In a slightly modified form, these polystyrene–polyisocyanopeptide block copolymers formed dynamic vesicles in water containing a small amount of THF. Removal of the organic solvent resulted in stable large vesicles in which enzymes could be included. Unexpectedly, substrate molecules are still able to permeate through the polymer membrane (see below) and can be converted by the enzymes present in the interior of the vesicle, in this way creating a type of nanoreactor (Fig. 3) [27].

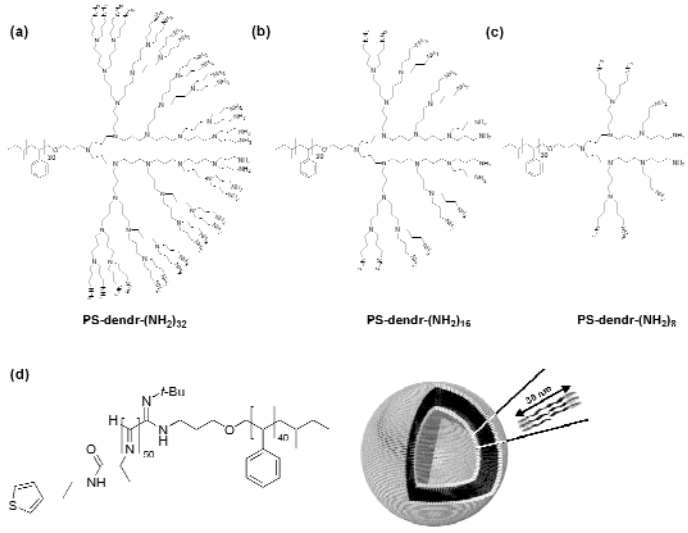

Fig. 3 Structures of vesicle-forming block copolymers. Polystyrene-dendrimer amphiphilic block copolymers that display generation-dependent aggregation behavior, i.e., into (a) spherical micelles; (b) micellar rods; and (c) vesicles. (d) Structure of polystyrene-poly(isocyanoalanyl-aminoethyl-thiophene) block copolymer (left) and schematic representation of the vesicles formed upon dispersal of this block copolymer in water (right).

Total polymer length dependence

According to a theoretical study of Safran et al. [28], vesicular phases can be stabilized by the curvature energy, i.e., vesicles are more stable with respect to the lamellar phase. Since the bending moduli of polymers increase with increasing molecular weight, the formation of vesicles should be easier in long-chain block copolymers compared to short-chain block copolymer systems. In block copolymer systems, due to the polydispersity, chains of different lengths will be unevenly distributed at the two sides of the bilayer, which will lead to vesicle formation. This segregation of polymer chains can also be used to thermodynamically stabilize polymersomes. Furthermore, this uneven distribution makes it

possible to preferentially segregate blocks on either the inside or outside of vesicles, which may have useful applications [29].

In order to determine whether the increase of molecular weight, i.e., the increase of the bending modulus (K), favors vesicle formation, series of PS-*b*-PAA block copolymers with different molecular weights and approximately the same ratio of the PAA block to the PS segment have been prepared [30]. Under certain conditions, the copolymer PS_{310}-*b*-PAA_{52} has been found to spontaneously form vesicles, whereas under the same conditions, polymers with smaller molecular weights form mainly open bilayers in coexistence with a small amount of vesicles. These studies confirm that long-chain copolymer systems have a stronger tendency to form polymersomes when compared to short-chain copolymers.

Additionally, in the aggregates described so far, the core-forming block mainly consists of PS, a material with a glass-transition temperature (T_g) of approximately 100 °C. This means, when the aggregates are isolated in water at room temperature this is substantially below the T_g. One question that arises is whether preservation of the morphology under various conditions, e.g., during electron microscopy studies, is due to this high T_g, resulting in a low mobility of the chains. Or whether other factors, such as hydrophobic interactions and core-chain stretching, preserve the morphology. In order to answer this question, aggregates from a range of polybutadiene-*block*-poly(acrylic acid) (PBD-*b*-PAA) polymers have been prepared [31]. Butadiene was chosen because during anionic polymerization the solvent polarity has a significant effect on the microstructure of polybutadiene (PBD) [32], i.e., on the T_g. It has been shown that aggregates of multiple morphologies (e.g., rod-like aggregates, LCMs, vesicles) can be obtained from all PBD-*b*-PAA block copolymers having a soft core-forming block (PBD). In these cases, the aggregates are able to retain their morphology even though the T_g of the core-forming block is much lower than the temperature at which the aggregates are formed and studied. Therefore, it appears that the morphology is mainly determined by the balance of forces between hydrophobic attraction and stretching of chains in the core-forming block, rather than by the T_g of the core-forming block.

PROPERTIES OF POLYMERSOMES

Polymersomes form a very distinct class of vesicles because the molecular weight of the building blocks is very large compared to that of liposome-forming lipids and other small-molecule surfactant systems. Mainly due to this large molecular weight, polymersomes possess remarkable properties, which will be discussed in the following sections.

Diffusion in polymersome bilayers

With fluorescence recovery after photobleaching (FRAP) [33], a common technique for membrane diffusion measurements, the lateral diffusion of the polymer chains in polyethylethylene-*block*-poly(ethylene oxide) (PEE_{40}-*b*-PEO_{37}) and polybutadiene-*block*-poly(ethylene oxide) (PBD_{130}-*b*-PEO_{80}) vesicles has been studied and compared to several liposomes [34]. For these measurements, fluorescent probes were covalently attached to the PEO's hydroxyl terminus. The vesicles were pulled into a glass micropipette, and the marker was rendered nonfluorescent via an intense photobleaching pulse of laser light. Due to lateral movement of the marker into the bleached region, fluorescence is subsequently recovered (Fig. 4).

For a series of liposomes, polymersomes, and bulk block copolymers [35] in the dense melt state, the diffusion coefficient at different temperatures was determined with FRAP in order to determine if Rouse dynamics are applicable. Rouse dynamics are only applicable to short, unentangled chains, and, therefore, the total hydrodynamic friction is just the cumulated friction on each of the N monomers or subsegments: $D_{\text{Rouse}} = k_B T/N\zeta$, where k_B is the Boltzmann constant. According to Rouse dynamics, the diffusion coefficient (D) is only dependent on the number of monomers and the monomeric friction fac-

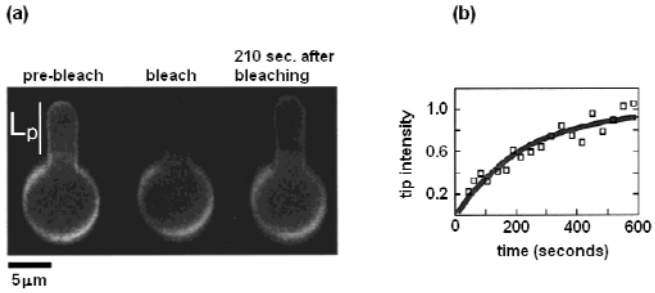

Fig. 4 FRAP method applied to a PEE_{40}-*b*-PEO_{37} vesicle pulled into a glass micropipette. (a) Laser bleaching of the fluorescent membrane creates a one-dimensional gradient on the projection of length (L_p). (b) Recovery of the tip intensity, normalized by the unbleached outer sphere. Reproduced from ref. [34] with permission from the American Chemical Society.

tor (ζ). Hence, if for system's ζ is the same, the diffusion coefficient, rescaled by total molecular weight (Rouse scaling), should have the same value. For a series of liposomes, polymersomes, and bulk block copolymers, the plot of the diffusion coefficient vs. temperature is depicted in Fig. 5.

From the experiments summarized in Fig. 5, it can be concluded that Rouse scaling is applicable to membrane mobilities of phospholipids as well as for PEE_{40}-*b*-PEO_{37} or comparable-sized copolymers (either in bulk or in vesicular phase). However, block copolymers with higher molecular weights appear to be less mobile than expected from any Rouse-type dynamics, indicating that reptation-type motions are possible due to chain entanglements. This means that the mobility of high-molecular-weight polymersomes ($M_n > M_e$; M_e = entanglement molecular weight) is very low compared to liposomes. Furthermore, the dynamics of polymer vesicles can be extrapolated to the dynamics of comparable copolymers in the dense melt state. This suggests that the hydrophobic membrane of the polymersomes is behaving like a fluid-like melt.

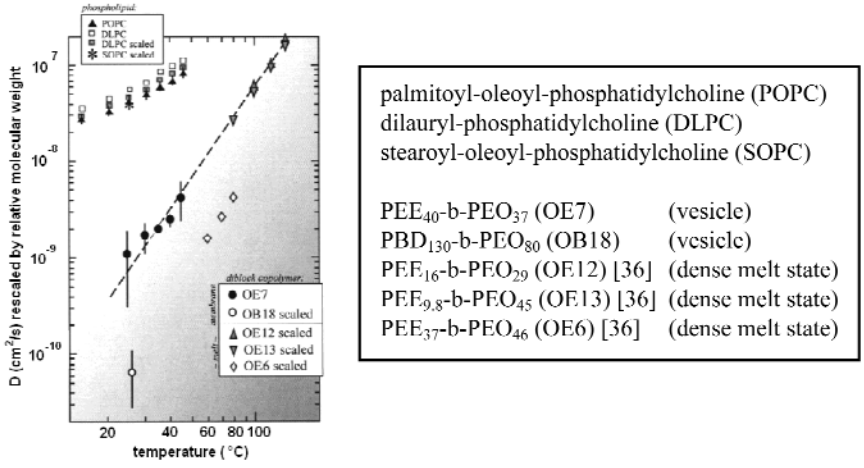

Fig. 5 Diffusion coefficient (D) of various phospholipids and diblock copolymers measured with FRAP method as a function of temperature. The phospholipids are all rescaled by total molecular weight with respect to POPC [e.g., $\tilde{D}_{DLPC} \equiv D_{DLPC}(M_{DLPC}/M_{POPC})$] and the diblock copolymers are all rescaled with respect to PEE_{40}-*b*-PEO_{37} (OE7). Reproduced from ref. [34] with permission from the American Chemical Society.

Vesicle morphologies

Owing to this low mobility of polymer chains in the aggregates, it is also possible to trap near-equilibrium and metastable morphologies. Therefore, a variety of vesicular morphologies have been obtained [37]. Among these polymer vesicular aggregates are new morphologies, which cannot be obtained from lipids or other small-molecule surfactants. Furthermore, it is possible to trap intermediate structures of morphological transitions [38], giving insight into the mechanism of these transitions.

Equilibrium morphologies

Vesicles are equilibrium structures under some conditions. When vesicles are prepared via the water addition (WA) method, at high water content, sufficient time should be allowed after each water addition to regain equilibrium because the chain dynamics are slow at high water content. If water addition is too fast, it is possible to freeze or quench nonequilibrium morphologies [6]. Small, uniform vesicles as well as large, polydisperse vesicles have been obtained under equilibrium conditions, as depicted in Fig. 6.

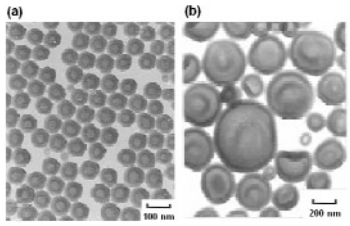

Fig. 6 Equilibrium vesicular structures; (a) small, uniform vesicles from PS_{410}-*b*-PAA_{13} [39]; and (b) large, polydisperse vesicles from PS_{390}-*b*-PAA_{41} [40]. Reproduced from refs. [39,40] with permission from the American Chemical Society.

For vesicles formed under equilibrium conditions, it has been shown that the size of the vesicles can be changed completely reversibly by changing the water content of the solvent (Fig. 7) [41], which confirms that these vesicles are indeed equilibrium structures under thermodynamic control. The reason for the increase in vesicle size in response to increasing water content is likely related to the increase in the interfacial energy of the system. This would drive the system to reduce the total interfacial area by increasing the vesicle size.

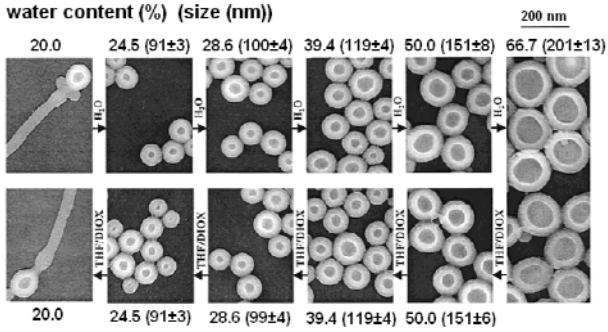

Fig. 7 PS_{300}-*b*-PAA_{44} vesicles in THF/dioxane (44.4/55.6)/water mixtures. The vesicle size can be changed reversibly in response to increasing or decreasing water contents. Reproduced from ref. [41] with permission from the American Chemical Society.

Detailed investigations of the mechanical aspects of the formation of these vesicles showed that small, uniform vesicles originate from rod-shaped structures [6,31]. These rod-shaped structures are converted into structures containing paddle-like protrusions, as can be seen in Fig. 7, for the transmission electron microscopy (TEM) images at 20 % water content. For large polydisperse vesicles, it is believed lamellae are intermediate structures, and that these lamellae bend until they close to form vesicles [37].

Nonequilibrium trapped morphologies

As mentioned above, owing to the polymer chain dynamics it is possible to freeze or quench nonequilibrium structures. Some of these vesicular structures cannot be obtained from phospholipids or other small-molecule surfactants owing to the high mobility of these molecules. Examples of such nonequilibrium polymer vesicular aggregates are depicted in Fig. 8.

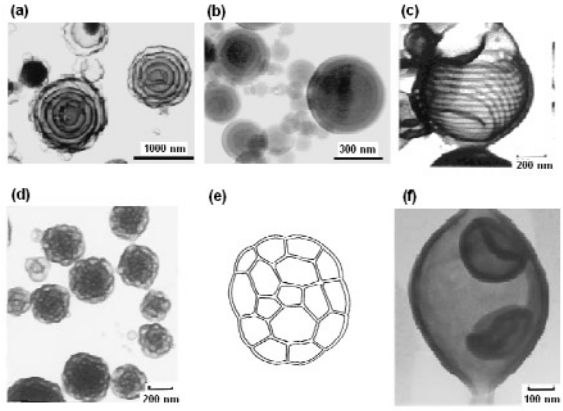

Fig. 8 Nonequilibrium trapped vesicular morphologies; (a) hollow concentric vesicles from PS_{132}-*b*-PAA_{20} [42]; (b) "onion"-type vesicles from polystyrene-*block*-poly(4-vinylpyridine decyliodide) (PS_{260}-*b*-$P(4\text{-}VPDecI)_{70}$) [42]; (c) tube-walled vesicle from PS_{125}-*b*-PEO_{43} [38]; (d) large compound vesicles (LCVs) from PS_{410}-*b*-PAA_{13} [39]; (e) schematic picture of the cross-section of a LCV in (d); and (f) entrapped vesicles from PS_{240}-*b*-PEO_{15} [11]. Reproduced from refs. [11,38,39] with permission from the American Chemical Society, and from ref. [42] with permission from Wiley Interscience.

Hydrophobic core thickness

A common feature of all natural membranes, despite the diversity in the used lipids, is that they all possess a hydrophobic core thickness that lies in a very narrow range of 3–4 nm [43]. However, the hydrophobic core thickness of polymersomes ranges from 3 nm (e.g., for PEO_5-PPO_{68}-*b*-PEO_5 [19]) up to ~200 nm (for polystyrene-*block*-poly(phenylquinoline) (PS_{300}-*b*-PPQ_{50}) [44]), depending on the composition, the molecular weight (M_n) and the degree of stretching of the core-forming block (S_c). For example, polymer vesicles of PEO_5-PPO_{68}-*b*-PEO_5 [19] have relative thin polymer membranes of 3–5 nm, compared to the 25 nm contour length of the PPO_{68}. These membranes are probably this thin because of the tendency for interfacial localization of the mid-block oxygen. Furthermore, the hydrophobic core thickness is dependent on the molecular weight of the core-forming block. For a series of PEE-*b*-PEO and PBD-PEO block copolymers, the increase in hydrophobic core thickness with molecular weight (M_n) has been demonstrated via direct imaging of the vesicles by cryo-TEM [45]. Based on these data, an experimental scaling relationship is found between the membrane thickness (d) and the hydrophobic molecular weight: $M_h \approx M_n(1 - f)$, where f is the hydrophilic volume fraction. This experimental scaling of $d \sim (M_h)^a$ leads to an exponent of $a \approx 0.5$, as illustrated in Fig. 9.

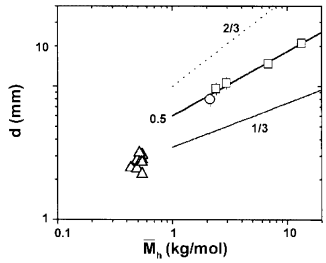

Fig. 9 Scaling of core thickness (d) with hydrophobic molecular weight (M_h). Data are shown for vesicles of various phospholipids (△), PEE_{37}-*b*-PEO_{40} (○), and the PBD-*b*-PEO series (□). Reproduced from ref. [45] with permission from the American Chemical Society.

In theory, fully stretched chains would give $a = 1$, and random coils would give $a = 1/2$. This factor 1/2 is based on the RMS (root mean square) end-to-end distance of a polymer chain in the unperturbed state, which is proportional to $N^{1/2}$ (N is the number of monomers). Since these block copolymers are expected to be in the strong segregation limit (SSL), a balance of interfacial tension and chain entropy would yield a scaling of $a = 2/3$. However, the best-fit scaling of $a = 0.5$ suggests that the polymer chains are relatively unperturbed from their ideal state.

Permeability of polymersome membrane

As mentioned in the previous section, the membrane thickness of polymersomes can exceed that of lipid membranes up to 65 times. This increased membrane thickness, together with the conformational freedom of the polymer chains, can lead to vesicles that are far less permeable to water compared to liposomes.

The water permeability has been studied for PEE_{37}-*b*-PEO_{40} vesicles with a hydrophobic wall thickness of approximately 8 nm [18]. In order to conduct permeability measurements, vesicles were prepared in 100 mOsm sucrose solution. Subsequently, a single vesicle was moved to a chamber with 120 mOsm sucrose solution. Due to the osmotic gradient between the inside and the outside of the vesicle, water starts to flow out of the vesicle, which leads to an increased projection length that was measured over time.

For the PEE_{37}-*b*-PEO_{40} block copolymer vesicles, the permeability coefficient (P_f) was measured to be 2.5 ± 1.2 μm/s. In contrast, phospholipid-based vesicles with acyl chain ≤18 carbon atoms typically have permeabilities in the fluid state of 25 to 100 μm/s. This means that polymersomes composed of PEE_{37}-*b*-PEO_{40} are at least 10 times less permeable to water when compared to conventional liposomes.

CONCLUSIONS AND OUTLOOK

From the first reports on the spontaneous formation of defined morphologies in (aqueous) dispersion by the self-assembly of block copolymers [21,25] until present studies, it is evident that block copolymer vesicles (i.e., polymersomes) have a wide range of potential applications. Compared to liposomes, polymer vesicles are substantially more stable and it is possible to vary parameters like block ratio, chemical composition, and (stereochemical) structure in order to define the properties of the materials obtained. Although the basic principles for the construction of polymersomes are only now in the process of being formulated [4,5], applications of these systems in the fields of drug delivery, gene transfection, and transmembrane transport have already been reported.

Combining the polymersome concept with biomacromolecules opens a new area in which the self-organizing properties of block copolymers can be combined with the functionality of enzymes

and/or other proteins. Initial steps in this direction have been taken by including enzymes in block copolymer vesicles, in this way constructing a nanometer-sized reactor [27], or by preparing vesicle forming block copolymers having a polypeptide block [51]. The use of a functional protein as the hydrophilic headgroup in combination with a synthetic polymer (e.g., polystyrene) as the hydrophobic tail with the aim of preparing giant amphiphilic macromolecules has been pioneered by Nolte [52]. Using both covalent and noncovalent coupling procedures, proteins (e.g., lipase, streptavidin, horse radish peroxidase) were connected with polystyrene to yield amphiphiles forming a variety of morphologies upon dispersal in water. Some of the enzyme containing aggregates retained part of their catalytic activity, exemplifying the great promise for the construction of biomimetic functional protein assemblies.

ACKNOWLEDGMENTS

The authors would like to thank the Chemical Council of the Netherlands Organization for Scientific Research (NWO-CW) for financial support for J.J.L.M.C. (VENI grant) and J.A.O. Prof. R. J. M. Nolte and Dr. A. E. Rowan are acknowledged for fruitful discussions.

REFERENCES

1. A. Halperin, M. Tirrell, T. P. Lodge. *Adv. Polym. Sci.* **100**, 31–71 (1992).
2. (a) E. L. Thomas, B. D. Alward, D. J. Kinning, D. C. Martin, D. L. Handlin, D. J. Fetters. *Macromolecules* **19**, 2197–2202 (1986); (b) J. Zhu, A. Eisenberg, R. B. Lennox. *J. Am. Chem. Soc*. **113**, 5583–5588 (1991); (c) E. L. Thomas, D. M. Anderson, C. S. Henkee, D. Hoffman. *Nature* **334**, 598–601 (1988).
3. D. J. Kinning, K. I. Winey, E. L. Thomas. *Macromolecules* **21**, 3502–3506 (1988).
4. D. E. Discher and A. Eisenberg. *Science* **297**, 967–973 (2002).
5. M. Antonietti and S. Förster. *Adv. Mater.* **15**, 1323–1333 (2003).
6. H. Shen and A. Eisenberg. *J. Phys. Chem. B* **103**, 9473–9487 (1999).
7. L. Chen, H. Shen, A. Eisenberg. *J. Phys. Chem. B* **103**, 9488–9497 (1999).
8. H. Shen, L. Zhang, A. Eisenberg. *J. Am. Chem. Soc.* **121**, 2728–2740 (1999).
9. S. M. Gravano, M. Borden, T. Von Werne, E. M. Doerffler, G. Salazar, A. Chen, E. Kisak, J. A. Zasadzinski, T. E. Patten, M. L. Longo. *Langmuir* **18**, 1938–1941 (2002).
10. K. Yu and A. Eisenberg. *Macromolecules* **29**, 6359–6361 (1996).
11. K. Yu and A. Eisenberg. *Macromolecules* **31**, 3509–3518 (1998).
12. S. J. Holder, R. C. Hiorns, N. A. J. M. Sommerdijk, S. J. Williams, R. G. Jones, R. J. M. Nolte. *Chem. Commun.* **14**, 1445–1446 (1998).
13. N. A. J. M. Sommerdijk, S. J. Holder, R. C. Hiorns, R. G. Jones, R. J. M. Nolte. *Macromolecules* **33**, 8289–8294 (2000).
14. J. Ding and G. Liu. *Macromolecules* **30**, 655–657 (1997).
15. J. Ding and G. Liu. *J. Phys. Chem. B* **102**, 6107–6113 (1998).
16. J. Ding and G. Liu. *Chem. Mater.* **10**, 537–542 (1998).
17. J. Ding, G. Liu, M. Yang. *Polymer* **38**, 5497–5502 (1997).
18. B. M. Discher, Y.-Y. Won, D. S. Ege, J. C.-M. Lee, F. S. Bates, D. E. Discher, D. A. Hammer. *Science* **284**, 1143–1146 (1999).
19. K. Schillén, K. Bryskhe, Y. S. Mel'nikova. *Macromolecules* **32**, 6885–6888 (1999).
20. A. Chouciar and A. Eisenberg. *Eur. Phys. J. E* **10**, 37–44 (2003).
21. L. Zhang and A. Eisenberg. *Science* **268**, 1728–1731 (1995).
22. L. Zhang and A. Eisenberg. *J. Am. Chem. Soc.* **118**, 3168–3181 (1996).
23. J. N. Israelachvili, D. J. Mitchell, B. W. Ninham. *J. Chem. Soc., Faraday Trans. 2* **72**, 1525–1568 (1976).

24. D. J. Mitchell and B. W. Ninham. *J. Chem. Soc., Faraday Trans. 2* **77**, 601–629 (1981).
25. J. C. M. Van Hest, D. A. P. Delnoye, M. W. L. P. Baars, M. H. P. Van Genderen, E. W. Meijer. *Science* **268**, 1592–1595 (1995).
26. J. J. L. M. Cornelissen, M. Fischer, N. A. J. M. Sommerdijk, R. J. M. Nolte. *Science* **280**, 1427 (1998).
27. D. M. Vriezema, J. Hoogboom, K. Velonia, K. Takazawa, P. C. M. Christianen, J. C. Maan, A. E. Rowan, R. J. M. Nolte. *Angew. Chem., Int. Ed.* **42**, 772 (2003).
28. S. A. Safran, P. Pincus, D. Andelman. *Science* **248**, 354–356 (1990).
29. (a) H. Shen and A. Eisenberg. *J. Phys. Chem. B* **103**, 9488–9497 (1999); (b) L. Luo and A. Eisenberg. *J. Am. Chem. Soc.* **123**, 1012–1013 (2001); (c) L. Luo and A. Eisenberg. *Angew. Chem., Int. Ed.* **41**, 1001–1004 (2002).
30. H. Shen and A. Eisenberg. *Macromolecules* **33**, 2561–2572 (2000).
31. Y. Yu, L. Zhang, A. Eisenberg. *Langmuir* **13**, 2578–2581 (1997).
32. Y. S. Yu, Ph. Dubios, R. Jérôme, Ph. Teyssié. *Macromolecules* **29**, 2738–2745 (1996).
33. D. Axelrod, D. E. Koppel, J. Schlessinger, E. Elson, W. W. Webb. *Biophys. J.* **16**, 1055–1069 (1976).
34. J. C.-M. Lee, M. Santore, F. S. Bates, D. E. Discher. *Macromolecules* **35**, 323–326 (2002).
35. M. W. Hamersky, M. A. Hillmyer, M. Tirrell, F. S. Bates, T. P. Lodge. *Macromolecules* **31**, 5363–5370 (1998).
36. M. A. Hilmyer and F. S. Bates. *Macromolecules* **29**, 6994–7002 (1996).
37. S. Burke, H. Shen, A. Eisenberg. *Macromol. Symp.* **175**, 273–283 (2001).
38. K. Yu, C. Bartels, A. Eisenberg. *Langmuir* **15**, 7157–7167 (1999).
39. L. Zhang and A. Eisenberg. *Macromolecules* **29**, 8805–8815 (1996).
40. Y. Yu, L. Zhang, A. Eisenberg. *Macromolecules* **31**, 1144–1154 (1998).
41. L. Luo and A. Eisenberg. *Langmuir* **17**, 6804–6811 (2001).
42. H. Shen and A. Eisenberg. *Angew. Chem., Int. Ed.* **39**, 3310–3312 (2000).
43. B. M. Discher, D. A. Hammer, F. S. Bates, D. E. Discher. *Curr. Opin. Colloid Interface Sci.* **5**, 125–131 (2000).
44. S. A. Jenekhe and X. L. Chen. *Science* **279**, 1903–1907 (1998).
45. H. Bermudez, A. K. Brannan, D. A. Hammer, F. S. Bates, D. E. Discher. *Macromolecules* **35**, 8203–8208 (2002).
46. D. E. Discher, N. Mohandas, E. A. Evans. *Science* **266**, 1032–1035 (1994).
47. C. A. Naumann, C. F. Brooks, C. G. Fuller, T. Lehmann, J. Rühe, W. Knoll P. Kuhn, O. Nuyken, C. W. Frank. *Langmuir* **17**, 2801–2806 (2001).
48. H. Aranda-Espinoza, H. Bermudez, F. S. Bates, D. E. Discher. *Phys. Rev. Lett.* **87**, 208301 (2001).
49. C. Nardin, Th. Hirt, J. Leukel, W. Meier. *Langmuir* **16**, 1035–1041 (2000).
50. B. M. Discher, H. Bermudez, D. A. Hammer, D. E. Discher, Y.-Y. Won, F. S. Bates. *J. Phys. Chem. B* **106**, 2848–2854 (2002).
51. (a) F. Chécot, S. Lecommandeux, Y. Gnanou, H.-A. Klok. *Angew. Chem., Int. Ed.* **41**, 1340 (2002); (b) H. Kukula, H. Schlaad, M. Antonietti, Förster. *J. Am. Chem. Soc.* **124**, 1658 (2002).
52. (a) J. M. Hannink, J. J. L. M. Cornelissen, J. A. Farrera, P. Foubert, F. C. De Schryver, N. A. J. M. Sommerdijk, R. J. M. Nolte. *Angew. Chem., Int. Ed.* **40**, 4732 (2001); (b) K. Velonia, A. E. Rowan, R. J. M. Nolte. *J. Am. Chem. Soc.* **124**, 4224 (2002); (c) M. J. Boerakker, J. M. Hannink, P. H. H. Bomans, P. M. Frederik, R. J. M. Nolte, E. M. Meijer, N. A. J. M. Sommerdijk. *Angew. Chem., Int. Ed.* **41**, 3239 (2002).